Clim Dyn (2011) 36:1207–1219
DOI 10.1007/s00382-010-0863-6

The relation of vegetation over the Tibetan Plateau to rainfall in China during the boreal summer

Zhiyan Zuo · Renhe Zhang · Ping Zhao

Received: 6 August 2009 / Accepted: 31 May 2010 / Published online: 17 June 2010

Abstract The relationship between vegetation on the Tibetan Plateau (TP) and summer (June–August) rainfall in China is investigated using the normalized difference vegetation index (NDVI) from the Earth Resources Observation System and observed rainfall data from surface 616 stations in China for the period 1982–2001. The leading mode of empirical orthogonal functions analysis for summer rainfall variability in China shows a negative anomaly in the area from the Yangtze River valley to the Yellow River valley (YYR) and most of western China, and positive anomalies in southern China and North China. This mode is significantly correlated with summer NDVI around the southern TP. This finding indicates that vegetation around the southern TP has a positive correlation with summer rainfall in southern China and North China, but a negative correlation with summer rainfall in YYR and western China. We investigate the physical process by which vegetation change affects summer rainfall in China. Increased vegetation around the southern TP is associated with a descending motion anomaly on the TP and the neighboring area to the east, resulting in reduced surface heating and a lower Bowen ratio, accompanied by weaker divergence in the upper troposphere and convergence in the lower troposphere on the TP. In turn, these changes result in the weakening of and a westward shift in the southern Asian High in the upper troposphere and thereby the weakening of and an eastward withdrawal in the western Pacific subtropical high. These features result in weak circulation in the East Asian summer monsoon. Consequently, enhanced summer rainfall occurs in southern China and North China, but reduced rainfall in YYR.

Z. Zuo (✉) · R. Zhang
State Key Laboratory of Severe Weather,
Chinese Academy of Meteorological Sciences,
No. 46 Zhong-Guan-Cun South Ave., Haidian District,
Beijing 100081, China
e-mail: zyzuo@cams.cma.gov.cn

P. Zhao
National Meteorological Information Centre, Beijing, China

1 Introduction

The nature of vegetation–climate interaction has been a focus of studies on climate sensitivity in the past two decades (Dickinson et al. 1998; Wang et al. 2007). It is known that the distribution of natural vegetation is governed by climate via factors such as precipitation, temperature, light, and CO_2 concentration (Nemani et al. 2003). Furthermore, recent studies have indicated that vegetation provides a feedback to climate via surface albedo, soil moisture, evapotranspiration via the exchange of heat and water, and other factors (Pielke et al. 1998; Kaufmann et al. 2003). Because the persistence of vegetation "greenness" is longer than 1–2 months, changes in terrestrial vegetation affect atmospheric circulation persistently, thereby modifying local, regional, or global climate at diurnal, seasonal, and long-term scales (Dickinson and Henderson-Sellers 1988; Lim et al. 2008).

The feedback of vegetation on temperature is complicated because of spatial variations in climate. For example, the northward expansion of grasslands over the southern Sahara and Arabian deserts may lead to local cooling (Foley et al. 1998). A cooling of about 1.8 K in northern latitudes during the growing season and a slight warming during the winter were associated with increased values of the normalized difference vegetation index (NDVI) (Bounoua et al. 2000). Liu et al. (2006) reported a significant positive correlation between surface temperature

anomalies and vegetation of the preceding month over boreal regions of southern Canada/northern United States, using a simple statistical method (Frankignoul et al. 1998). Finally, the vegetation feedback on precipitation has been found to be positive under wet soil-moisture anomalies during summer (Kim and Wang 2007).

The relationship between vegetation change and the East Asian climate has also received attention in recent years. For example, the desertification of Inner Mongolian grasslands has shown a marked increase during the past 40 years, which could weaken monsoonal circulation and reduce local rainfall (Xue 1996). A recent increase in the frequency of flood events within the Yangtze–Huaihe River valleys and intensification of droughts in North China may reflect the joint effects of desertification and degradation of northern grassland and southern evergreen broadleaf forests (Zheng et al. 2002). Zhang et al. (2005) showed that change in vegetation cover over northern China and surrounding areas has a significant influence on summer precipitation over China. Based on a numerical model, Chen et al. (2009) simulated the impact of different types of vegetation cover in western China on regional circulation. The authors found that anomalous anti-cyclonic circulation is centered over mid-latitude Asia, resulting in increased rainfall occurred over northwestern China in the 1990s relative to the 1970s.

The Tibetan Plateau (TP), which has an average altitude of about 4,000 m and acts as an elevated heating source in summer, plays an important role in atmospheric circulation via orographic and thermal forcings (e.g., Ye and Gao 1979; Ye and Wu 1998). Interannual and inter-decadal variability in the Asian summer monsoon and rainfall are closely related to anomalous heating over the TP (Li and Yanai 1996; Zhao and Chen 2001a, b). With the melting of snow and increasing temperature over the TP during the warm season, vegetation becomes denser, covering most of the land surface and attaining a peak during the growing season over the entire TP (Ding et al. 2007).

Previous studies have examined the influence of vegetation on the TP on rainfall of the East Asian monsoon. For example, Wang et al. (2009) examined the inter-decadal relationship between Tibetan vegetation and rainfall over eastern China in the boreal spring, finding that increased vegetation on the TP could enhance (reduce) spring rainfall north (south) of the Yangtze River. Furthermore, Hua et al. (2008) reported that vegetation over the TP correlated with the pattern of rainfall anomalies in China during July. Although these previous studies noted a possible relationship between Tibetan vegetation and rainfall in China, the relevant physical processes remain unknown.

The variability of summer rainfall over China correlates not only with ocean–atmosphere interactions, but also with land–atmosphere interactions that play a key role in the anomalies of the East Asian summer monsoon and thereby in rainfall variability over China (e.g., Yang and Lau 1998; Yu et al. 2001; Zhu and Wang 2001; Li et al. 2002; Xue et al. 2003; Zhu et al. 2007). Consequently, it is important to determine whether land–atmosphere interaction over Tibet (including Tibetan vegetation) is related to variability in summer rainfall over China. This study seeks to answer this question based on an analysis of NDVI data collected by the advanced very high resolution radiometer (AVHRR) housed on board the National Oceanic and Atmospheric Administration (NOAA) satellite, and station-observed rainfall from the National Meteorological Information Centre of China, with the aim of examining the relationship between the extent of summer vegetation over the TP and summer rainfall in China, as well as the relevant physical mechanisms.

The remainder of this paper is organized as follows. Section 2 describes the datasets and methods. The characteristics of summer rainfall variation in China and its relationship with vegetation over the TP are discussed in Sects. 3 and 4, respectively. In Sect. 5, we investigate the physical processes that underlie the influence of TP vegetation on rainfall. Finally, the main conclusions and a discussion are given in Sect. 6.

2 Data and methods

Satellite remote sensing has been used in previous studies to monitor vegetation dynamics (Tucker and Sellers 1986; Gutman 1991). Within the leaf, radiation may be absorbed or scattered, depending on its wavelength (Tucker and Miller 1977); consequently, vegetation strongly absorbs visible light, using the energy for photosynthesis, and strongly reflects near-infrared radiation. The NDVI exploits this response via the following equation:

$$\mathrm{NDVI} = \frac{L_2 - L_1}{L_2 + L_1},$$

where L_1 and L_2 are the visible and near-infrared land surface reflectance values, respectively, as obtained from channels 1 and 2 of the AVHRR housed on board NOAA satellites. Theoretically, NDVI values range from -1 to 1, and are closely related to the fraction of photosynthetically active radiation absorbed by the green parts of vegetation. In general, increased photosynthetic activity corresponds to higher values of NDVI. Temporal and spatial consistency in raw AVHRR NDVI data are compromised by sensor degradation, clouds, viewing geometry, and atmospheric effects (Goward et al. 1991). Consequently, corrections are applied to NDVI datasets to account for some of these effects and to improve the spatial and temporal integrity of the data (Los 1998). The present study analyzes monthly NDVI data at 1° latitude × 1° longitude resolution for the

period 1982–2001, as obtained from the Goddard Space Flight Center. Previous studies have shown that NDVI can be used to assess variability in Tibetan vegetation (Hua et al. 2008; Wang et al. 2009).

Data on air temperature, winds, and geopotential heights are from the National Centers for Environmental Prediction–National Center for Atmospheric Research (NCEP-NCAR) reanalysis version 1 output. We use empirical orthogonal function (EOF) analysis to examine the dominant modes of the summer rainfall variation in China. In addition, correlation and composite analyses are used to reveal the relationship between vegetation on the TP and rainfall in China, assessed using Student's t test.

3 Summer rainfall variability in China

The EOF analysis is applied to analyze the temporal and spatial features of summer (June–August) rainfall variation over China for the period 1982–2001. Figure 1 shows the first leading mode of normalized summer rainfall and the corresponding time series. The variance percentage explained by the first leading mode is 13.3%. The variation in summertime rainfall in southern China and North China has the opposite sign to that in the area from the Yangtze River valley to the Yellow River valley (YYR) and most of western China. In eastern China (east of 105°E), the center of variation in summertime rainfall occurs in YYR, southern China, and part of North China, with the maximum variation exceeding half a standard deviation. Figure 1b show the normalized time series of the first EOF mode of summer rainfall (hereafter RI). RI shows strong interannual variability, with the variation exceeding one standard deviation in eight of the 20 years.

4 Relationship between summer rainfall and vegetation on the TP

Figure 2a shows the distribution of the correlation coefficient between RI and summer NDVI over the Asian continent. The same data are shown in Fig. 2b, but with inter-decadal variations filtered out. Summer rainfall in China shows a marked positive correlation with NDVI over the southern TP and surrounding regions. In other words, increased NDVI around the southern TP corresponds to more rainfall in southern China and North China, and corresponds to less rainfall in YYR.

It should be noted that the above pattern of the summer rainfall variation showed an inter-decadal shift at around the early 1990s. Anomalous rainfall in southern China was mainly negative before the 1990s, but positive afterward. This finding is consistent with the results of Zhang et al. (2008), who reported that the distribution of summer rainfall over eastern China showed a marked transformation from the 1980s to the 1990s. However, after removing the inter-decadal variability in RI using a nine-point smoothing algorithm (using a 5-point smoothing algorithm at both the ends of RI), the spatial distribution of the area with a significant correlation in Fig. 2b is generally similar to that in Fig. 2a. Thus, this relationship is more pronounced on the interannual scale than on the inter-decadal scale.

To confirm the relationship between NDVI around the southern TP and the main pattern of summer rainfall variability in China, we obtained the average NDVI in the southern TP (24°–33°N, 75°–105°E) for elevations above 1,000 m (hereafter VSTP). Figure 3 shows the normalized time series of RI, VSTP, and rainfall averaged over southern China (south of 27°N, east of 105°E) and YYR (30°–35°N, 105°–120°E), respectively. The leading EOF mode of summer rainfall represents the variability in rainfall in both southern China and YYR, with a correlation coefficient of 0.81 between RI and rainfall in southern China (exceeding the 0.01 significance level) and a coefficient of −0.74 between RI and rainfall in YYR (exceeding the 0.01 significance level). As expected, a marked correlation is observed between VSTP and RI (correlation coefficient 0.72, significant at the 0.01 level). Summer rainfall in southern China and YYR shows significant correlations with VSTP, yielding correlation coefficients of 0.51 and −0.58, respectively. In general, higher VSTP corresponds to more summer rainfall in southern China and reduced rainfall in YYR, indicating that enhanced vegetation around the southern TP may have a strong influence on summer rainfall in China.

Figure 4a shows the climatology of summer NDVI around the southern TP for the period 1982–2001. It is evident that most of the TP is covered by vegetation in summer. We calculated composites of VSTP for 4 years with positive anomalies (1984, 1990, 1994, and 1997) and 4 years with negative anomalies (1982, 1983, 1987, and 1998). Clearly, the differences between the high vegetation around the southern TP (hereafter HV) years and low vegetation around the southern TP (hereafter LV) years are statistically significant (Fig. 4b), with the difference exceeding 0.1 over most of the southeastern TP. Below, we consider the physical processes by which vegetation around the southern TP affects summer rainfall in China.

5 Relationship between atmospheric circulation and vegetation anomalies over the TP

The Asian monsoon system is closely related to the heating condition of the land surface over the TP. Wu et al. (2002) suggested that near-surface heating and related vertical

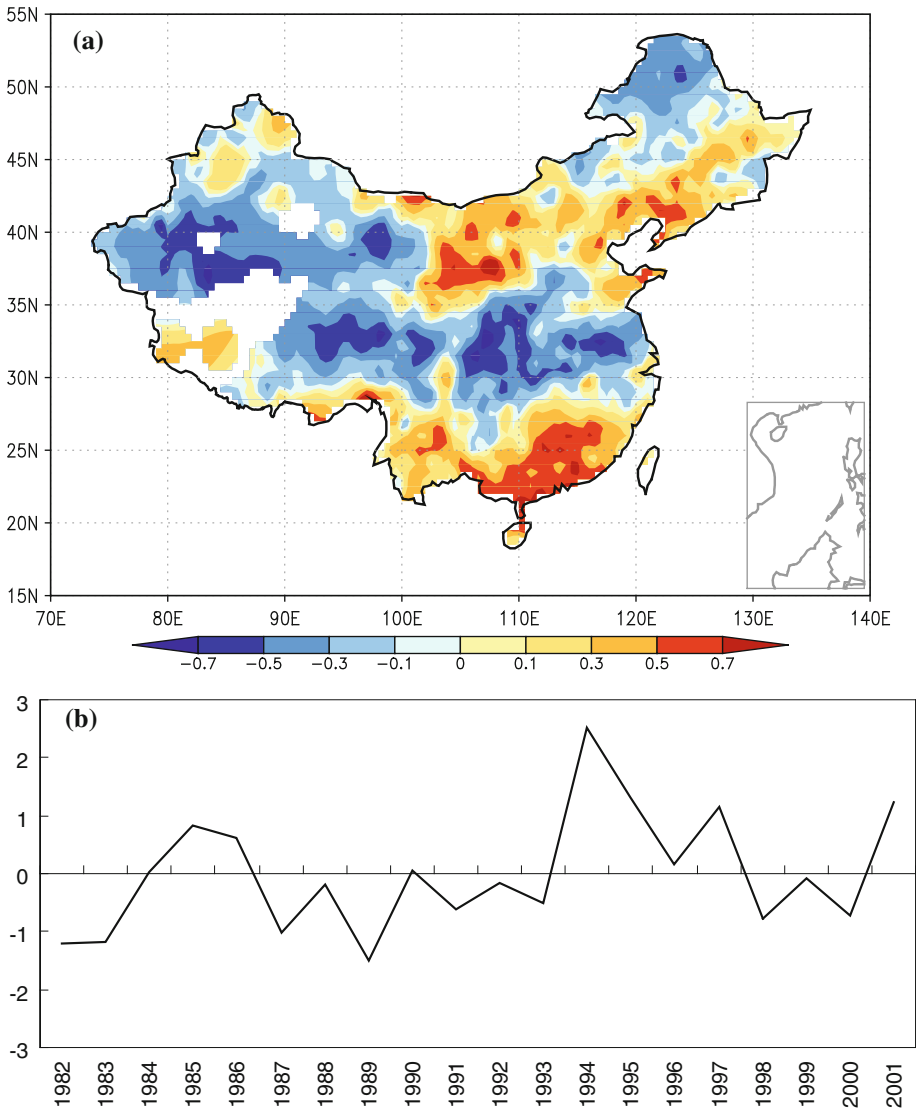

Fig. 1 **a** Spatial distribution of the first EOF mode of normalized summer rainfall in China for the period 1982–2001 (the explained variance of the leading mode is 13.3%). **b** Time series of the first EOF mode of normalized summer rainfall. In **a**, **b** units are one standard deviation

motion over the TP have important influences on the maintenance of summer circulation over the TP. In this section, we investigate the way in which the vegetation anomaly over the southern TP affects circulation over East Asia and rainfall in China.

5.1 Surface heating

To explore the effect of VSTP on atmospheric circulation, we first examine surface heating over the TP associated with anomalous VSTP. Figure 5a shows the composite difference of the amount of sensible and latent heat flux around the southern TP between HV and LV. Negative anomalies cover most of the southern TP, with a maximum difference of -10 W m^{-2}. In others words, greater vegetation over the southern TP results in reduced surface heating. Thus, increased vegetation acts as an extra heat sink in summer. The amount of vegetation changes not only the amount of surface sensible and latent heat fluxes, but also their relative magnitudes; i.e., the Bowen ratio (Fig. 5b). Increased VSTP is associated with a lower Bowen ratio over the southern TP, with a maximum difference between HV and LV of -0.4. These findings indicate that enhanced vegetation around the southern TP is associated with reduced surface heating and a lower Bowen ratio, generally resulting in a colder atmosphere.

The composite difference between HV and LV in terms of vertically integrated air temperature throughout the entire troposphere (from 600 to 100 hPa based on the TP height) over the southern TP is strongly negative (Fig. 6a). Thus, increased vegetation around the southern TP is accompanied by colder air in the troposphere that arises from a change in surface heating. Furthermore, we calculated the composite difference of longitude–height air temperature along 30°N latitude (Fig. 6b). Clearly, increased vegetation around the southern TP in summer is associated with a

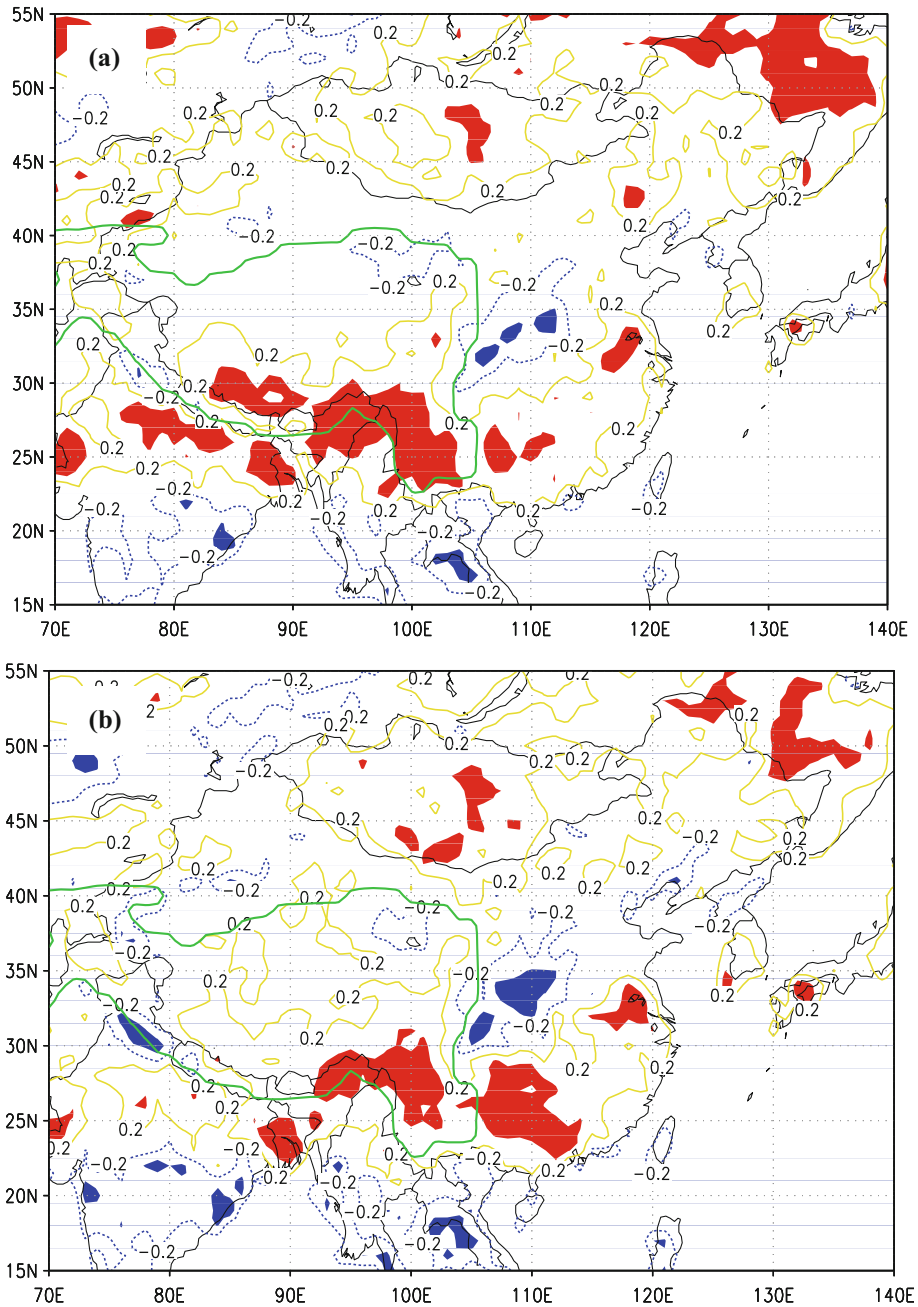

Fig. 2 **a** Spatial distribution of the correlation coefficient between the time series of the first EOF mode of normalized summer rainfall in China and NDVI around the southern TP (only the 0.2 and −0.2 isolines are shown). **b** Same as in **a**, but with inter-decadal variability filtered out. In **a**, **b** the *thick green line* indicates the 1,000 m topographic contour, and the *shaded areas* indicate that the correlation exceeds the 0.05 significance level (*red* indicates a positive correlation; *blue* indicates a negative correlation)

significantly colder atmospheric column in the middle and upper troposphere, consistent with the findings of Zheng et al. (2002), who reported that air temperature decreases in the warm season because of increased vegetation. The present results suggest that greater vegetation in the warm season can reduce the amount of heating at the surface, thereby affecting the air temperature over the TP, which in turn modulates the regional climate.

5.2 Upper-tropospheric South Asian high

In the climatology of the 100-hPa geopotential height (Fig. 7a), the South Asia high (SAH), centered near the TP, is a huge system that covers most of the subtropics in the eastern Northern Hemisphere. Figure 7b, c shows a composite geopotential height chart at 100 hPa for HV and LV, respectively. The SAH center extends westward to the Iranian Plateau (60°–80°E) in HV, whereas it extends eastward to the TP (80°–100°E) in LV. In addition, SAH is more robust in LV than in HV. Previous numerical simulations (Zhao et al. 2008, 2009) revealed that stronger (weaker) heating on the TP corresponds to an increase (decrease) in tropospheric temperature over the TP, with a stronger (weaker) SAH and ascending (descending) motion over the TP. Thus, in the present study, the decrease in tropospheric temperature and associated SAH variations can be

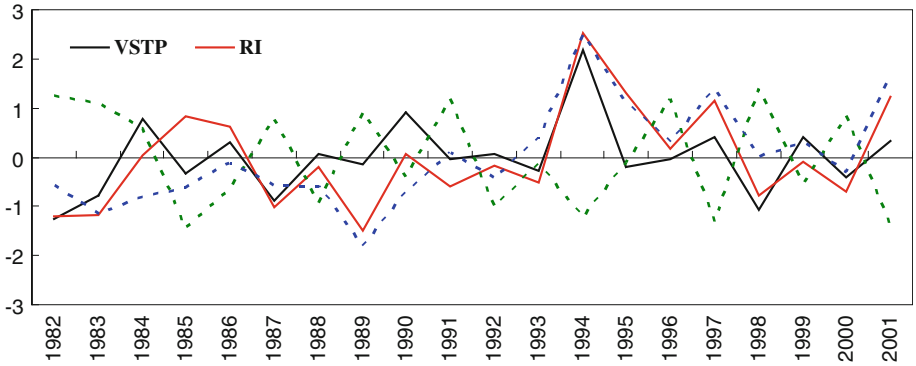

Fig. 3 Time series of the first EOF mode of normalized summer rainfall in China (RI *solid red line*), normalized NDVI around the southern TP (24°–33°N, 75°–105°E, elevations above 1,000 m; VSTP *solid black line*), and normalized summer rainfall in southern China (south of 27°N, east of 105°E; *dashed blue line*) and in the area from the Yangtze River valley to the Yellow River valley (30°–35°N, 105°–120°E; *dashed green line*)

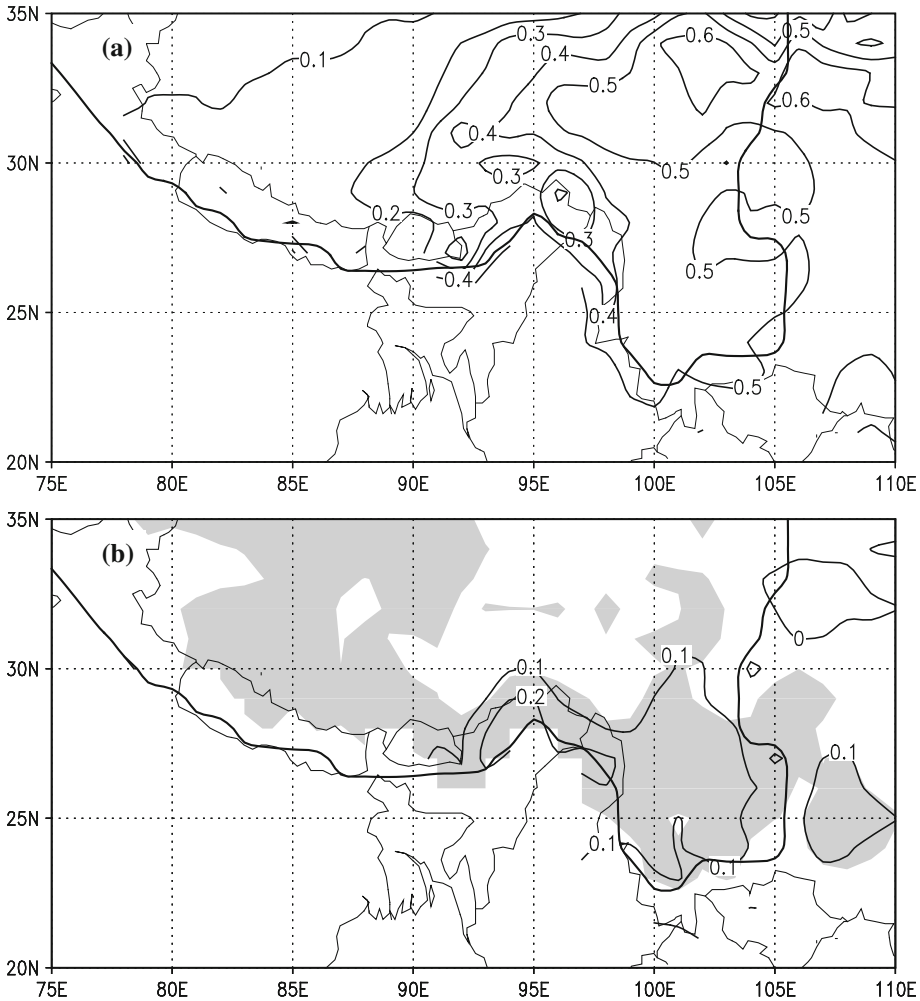

Fig. 4 **a** Climatology of NDVI around the southern TP in summer for the period 1982–2001, **b** composite difference between HV and LV in terms of NDVI in summer (interval is 0.1). *Shading* in **b** indicates that the composite difference exceeds the 0.05 significance level. The *thick black line* in **a**, **b** indicates the 1,000 m topographic contour

considered as a response of the atmosphere to reduced surface heating associated with increased vegetation over the southern TP. Previous studies reported that when SAH is in a more westward position than normal, the East Asian summer monsoon is weak, with less summer rainfall over YYR (Zhao and Chen 2001a; Wu et al. 2002; Zhang et al. 2002).

5.3 Middle- and lower-tropospheric circulation

Heating of the TP can influence the western North Pacific subtropical high (WPSH) during summer (Zhao and Chen 2001a). Figure 8 shows a composite of 500-hPa geopotential height for HV and LV, with WPSH indicated by the

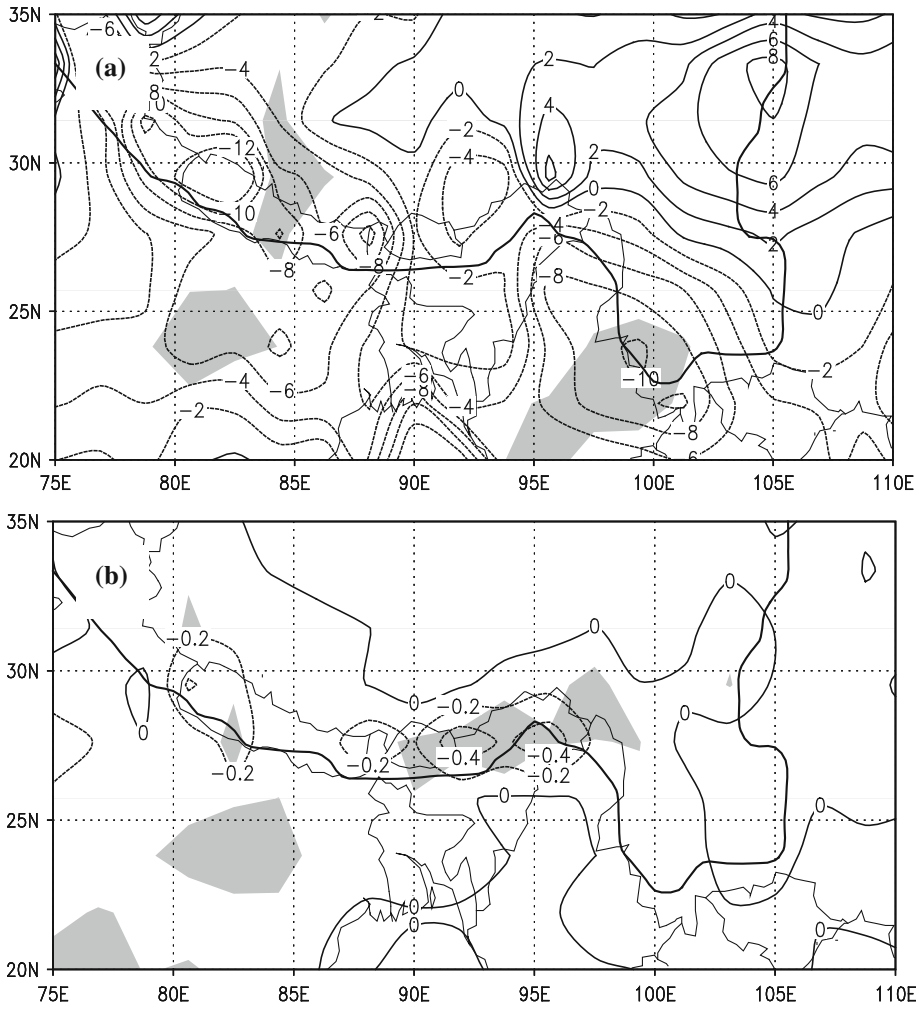

Fig. 5 Composite difference between HV and LV in terms of **a** the amount of surface sensible and latent heat flux (interval is 2 W m^{-2}) and **b** the Bowen ratio. *Shading* in **a**, **b** indicates that the composite difference exceeds the 0.05 significance level. The *thick black line* in **a**, **b** indicates the 1,000 m topographic contour

5,860, 5,870, and 5,880 gpm contours. In the case of low vegetation, the 5,860 gpm contour extends westward beyond 100°E, whereas in the case of high vegetation it is confined to east of 120°E. The increase in vegetation is accompanied by the weakening and eastward withdrawal of WPSH. These results show that increased vegetation corresponds to not only a more westward SAH center, but also weakening of WPSH.

Zhao et al. (2009) reported that anomalously strengthened summer SAH can influence ocean–atmosphere interactions in the Pacific via eastward propagation of wave energy along the waveguide of the westerly jet stream, resulting in an increase in upper-tropospheric geopotential height over the subtropics of the North Pacific and in turn an increase in low-level geopotential height over the extratropical North Pacific. This mechanism may explain the connection between vegetation around the southern TP and WPSH. In other words, greater vegetation around the southern TP corresponds to the weakening of and a westward shift in SAH, and thereby the weakening and eastward withdrawal of WPSH via weakening of the propagation of wave energy downstream along the westerly jet stream. Previous studies reported that a westward SAH and a weaker, eastward WPSH are generally associated with a negative anomaly in summer rainfall in YYR, and a positive anomaly in rainfall in southern China (Wu et al. 2003; Zhang and Tao 2003), which is consistent with the present results.

Climatologically, a trough extends from the TP to southern China, deflected by the TP in the low to middle troposphere and affected by heating in the TP (Ye and Gao 1979). Moreover, because the low-level southwest monsoon over eastern China appears east of the trough and west of WPSH during summer, the trough anomaly affects the intensity of the East Asian summer monsoon. Figure 9 shows the climatology 850-hPa geopotential height and the composite difference of 850-hPa horizontal wind between HV and LV. A significant northerly wind anomaly extends from the southeastern TP to southern China, while a significant southerly wind anomaly in North China, as well as a strong westerly wind anomaly, occurs south of 20°N. A cyclonic anomaly is observed over southern China and a

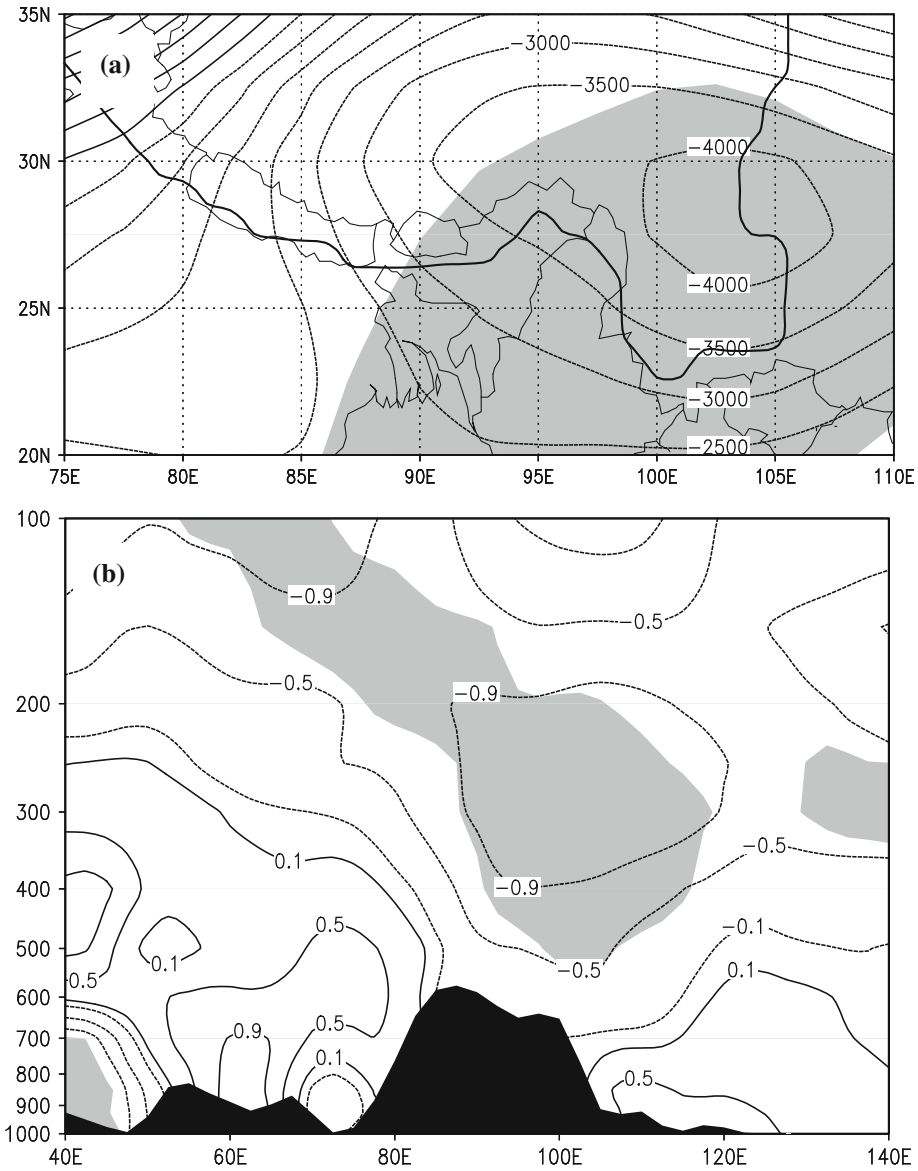

Fig. 6 **a** Composite difference between HV and LV in terms of the vertically integrated air temperature from 600 to 100 hPa (interval is 500°C × kg × m^{-2}). **b** Longitude–height section of the composite difference between HV and LV in terms of air temperature along 30°N (interval is 0.4°C). *Gray shading* in **a**, **b** indicates that the composite difference exceeds the 0.05 significance level. The *thick black line* in **a** indicates the 1,000 m topographic contour and the *black shaded areas* in **b** show topography

divergence anomaly occurs over YYR, which represent favorable conditions for enhanced rainfall in southern China and reduced rainfall in YYR. The anomalous westerly over the Indian monsoon region indicates greater water vapor transport from the Indian monsoon region to the East Asian monsoon region, which corresponds to reduced rainfall in YYR and enhanced rainfall in North China (Zhang 2001).

5.4 Vertical motion

According to static equilibrium, a cold air column is accompanied by shrinking and sinking. The lower air temperature due to increased vegetation acts to limit the robust ascending motion of the atmosphere over the TP in summer. Figure 10a shows a longitude–height section of the composite difference between HV and LV of vertical circulation along 30°–35°N. As expected, a significant anomalous descending motion appears over the eastern TP and adjacent regions to the east.

Figure 10b, c shows the composite differences between HV and LV in terms of wind and divergence at 200 and 600 hPa, respectively. In Fig. 10b, anomalous convergence occurs over the TP (convergence centre of 5 × 10^{-7} s^{-1}), consistent with the anomalous descending motion. Consequently, a strong anomalous cyclonic circulation at 200 hPa appears over the TP, Indochina, and southern China, with its center over the southeastern TP; an anomalous westerly wind prevails to the south of the anomalous centre. Meanwhile, strong anomalous divergence appears around the Iranian Plateau, consistent with the anomalous ascending motion over the Iranian Plateau seen in Fig. 10a.

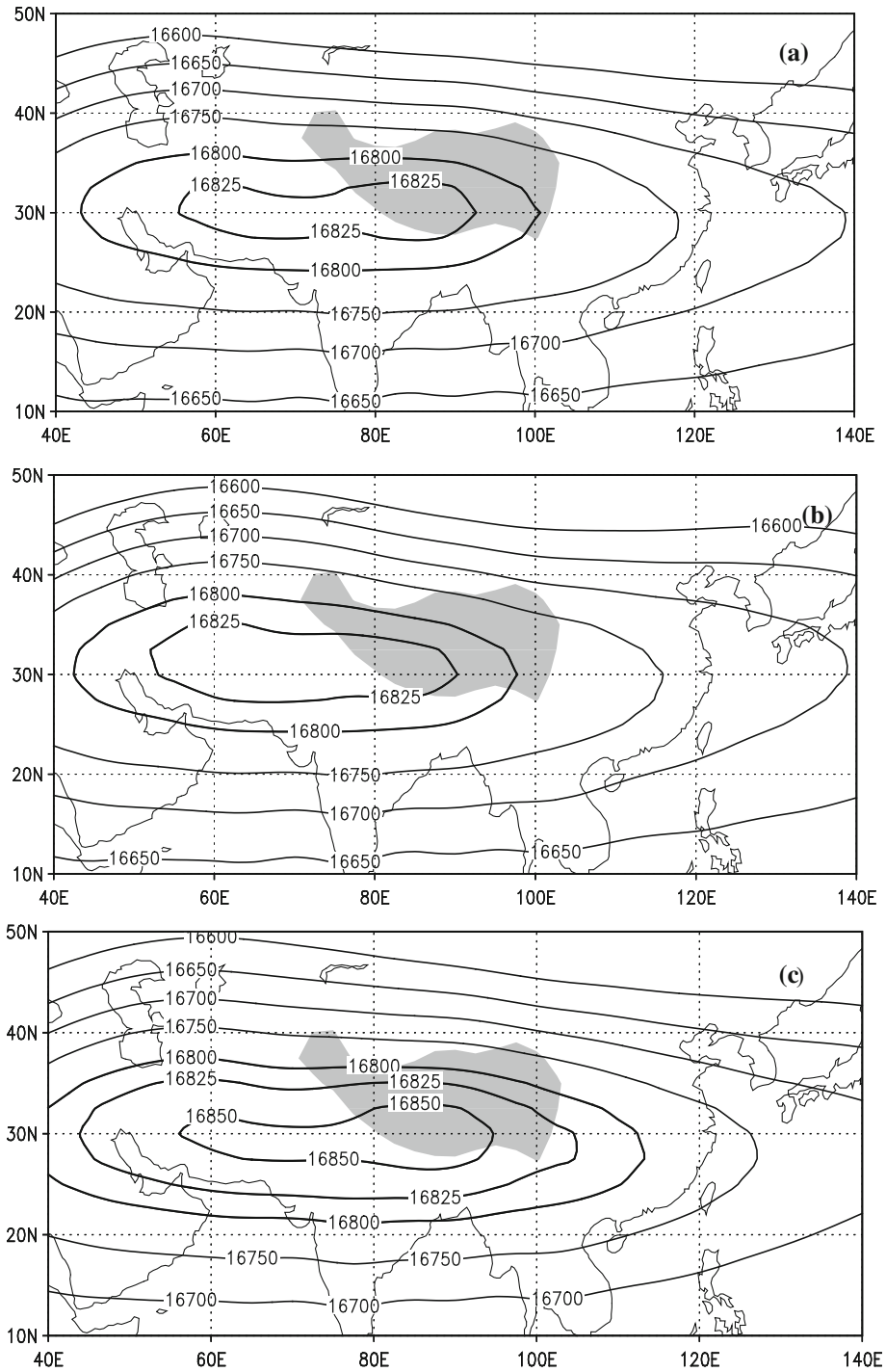

Fig. 7 **a** Climatology of summer 100-hPa geopotential height (unit: gpm), the composite summer 100-hPa geopotential height (unit: gpm) in the case of **b** HV and **c** LV for the period 1982–2001 (intervals are 25 and 50 gpm). *Shading* indicates areas in which the TP exceeds 3,000 m in altitude

Corresponding to the anomalous upper-tropospheric cyclonic convergence, an anomalous anti-cyclone occurs over the TP in the low-level wind field, accompanied by local low-level divergence anomalies (divergence centre of 15×10^{-7} s^{-1}; Fig. 10c), indicating weakened low-level convergence. Clearly, the anomalous descending motion associated with increased vegetation around the southern TP does not favor divergence in the upper troposphere. Consequently, both the upper-level anti-cyclonic circulation and the low-level cyclone are weakened over the TP.

Figure 11 shows a latitude–height section of the composite difference of vertical circulation along 100°–120°E between HV and LV. Corresponding to increased VSTP, an anomalous descending motion occurs in the entire troposphere over YYR, diverging at low levels. The anomalous ascending motion occurs over 20°–30°N and 35°–40°N;

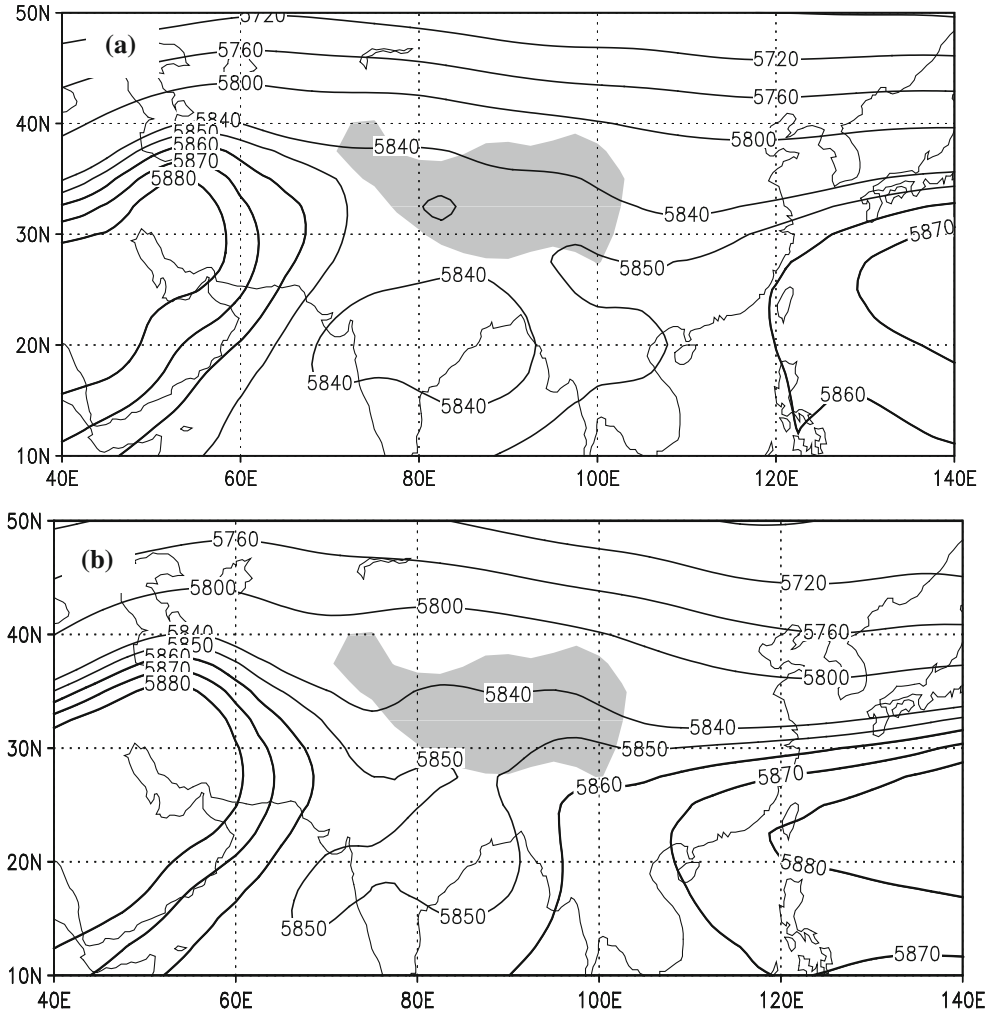

Fig. 8 Composite of 500-hPa geopotential height (gpm) in the case of **a** HV and **b** LV (intervals are 40 and 10 gpm). *Shading* indicates areas in which the TP exceeds 3,000 m in altitude

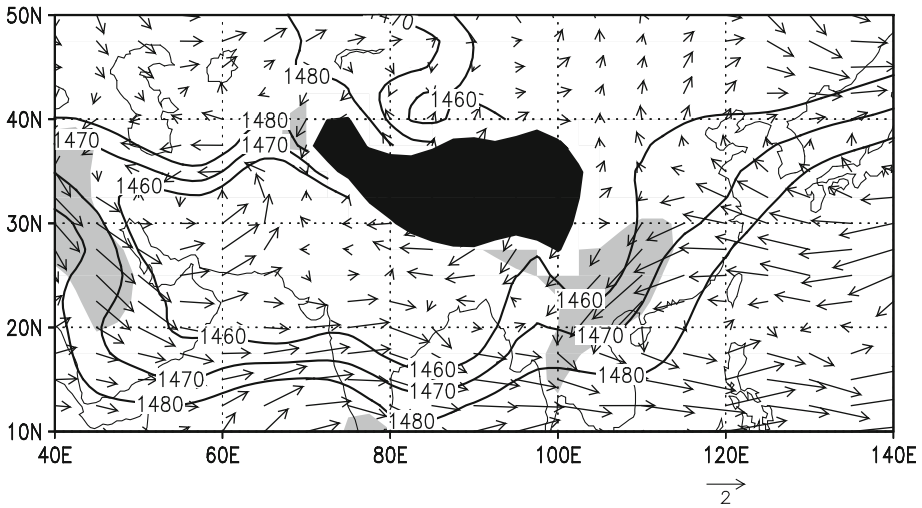

Fig. 9 Composite difference of horizontal wind at 850 hPa (vectors; m s^{-1}) between HV and LV and climatology of geopotential height (contours; gpm) during 1982–2001. *Gray shading* indicates that the composite difference of the meridional wind exceeds the 0.05 significance level. *Black shaded areas* indicate areas in which the TP above 3,000 m in altitude

i.e., the air mass over the eastern TP and neighboring regions to the east sinks down between 30°N and 35°N, diverging in the lower troposphere and rising up over southern China and North China. This pattern may lead to positive rainfall anomalies in the two areas, with reduced rainfall over YYR.

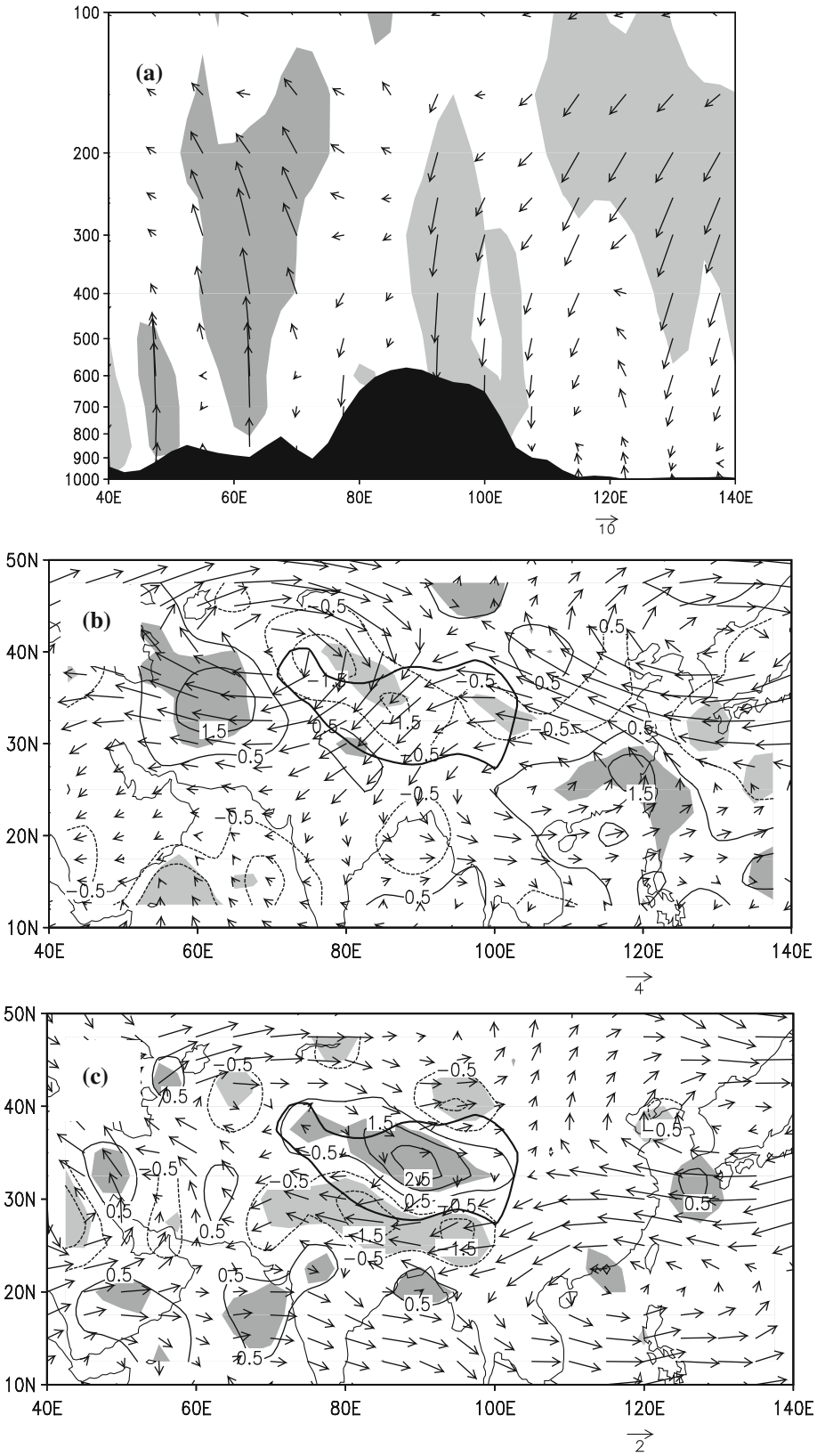

Fig. 10 **a** Longitude–height section of the composite difference between HV and LV in terms of vertical circulation (zonal wind; m s^{-1}; *p*-velocity; $\times 10^{-3}$ Pa s^{-1}). **b** Composite differences in horizontal winds (vectors; m s^{-1}) and divergence (contours; $\times$ 10^{-6} s^{-1}) at **b** 200 hPa and **c** 600 hPa. *Gray shading* in **a** indicates that the composite difference of velocity exceeds the 0.05 significance level; *grey shading* in **b**, **c** indicates that the composite difference of divergence exceeds the 0.05 significance level. The *black area* in **a** shows topography and the thick solid line in **b**, **c** is the 3,000 m topographic contour

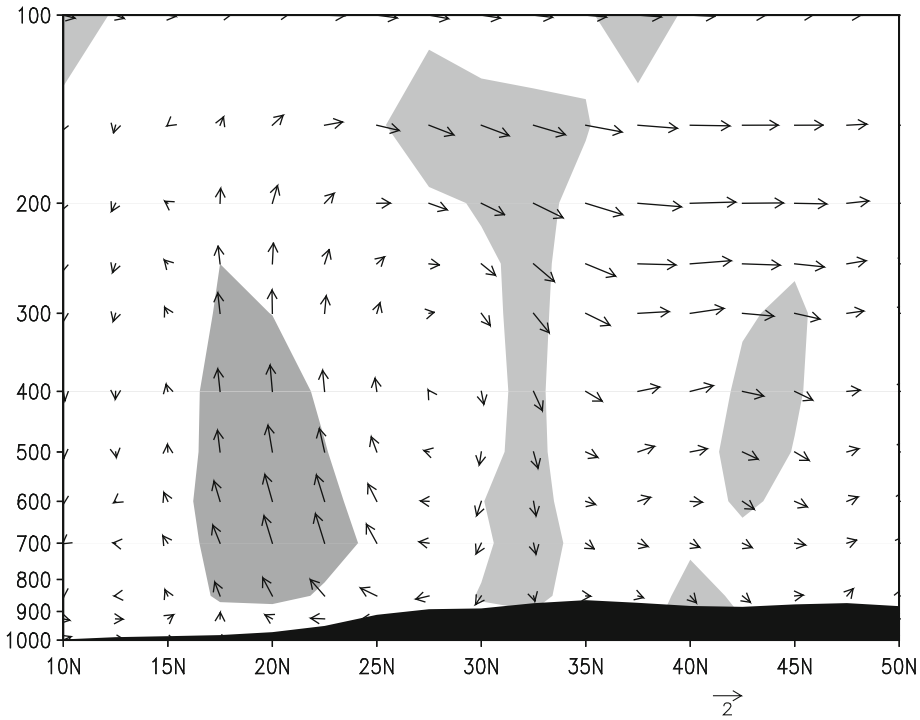

Fig. 11 Latitude–height section of the composite difference between HV and LV in terms of vertical circulation (meridional wind: m s^{-1}; *p*-velocity: $\times 10^{-2}$ Pa s^{-1}) along 100°–120°E. The *black area* shows topography. *Gray shading* indicates that the composite difference of velocity exceeds the 0.05 significance level

6 Summary and discussion

This study employed the NDVI and rainfall data for the period 1982–2001 in examining the relationship between the leading pattern of the summer rainfall variation over China and vegetation over East Asia. The first EOF mode of summer rainfall in China shows a negative anomaly in YYR and a positive anomaly in southern China and North China. This leading pattern correlates significantly with the summer NDVI around the southern TP. In the case of enhanced vegetation around the southern TP, summer rainfall tends to increase in southern China and North China, and decrease in YYR. This relationship between vegetation and summer rainfall is well explained in terms of atmospheric circulation.

During summer, when greater vegetation occurs over the southern TP, surface heating and the Bowen ratio are reduced over the TP, resulting in anomalous descending motion over the TP, which in turn weakens the upper-tropospheric divergence and lower-tropospheric convergence, accompanied by weakening of upper-level anti-cyclonic circulation and the development of a low-level anomalous anti-cyclone over the TP. In turn, this leads to a westward shift of the SAH to the Iranian Plateau, and the WPSH is weakened and moves eastward, corresponding to weak circulation in the East Asian summer monsoon. Corresponding to higher NDVI values around the southern TP, an anomalous northerly wind prevails over southern China and an anomalous southerly wind occurs over North China. The anomalous ascending motion appears in the entire troposphere over southern China and North China, with anomalous descending motion appearing over YYR. As a result, rainfall is enhanced in southern China and North China, and is reduced in YYR. However, our results here are from data diagnoses. It should be noted that further analysis with numerical experiments will be necessary to approve the relationship between vegetation over the TP and rainfall over China during summertime.

Acknowledgments We thank the National Meteorological Information Centre of the China Meteorological Administration for providing precipitation data for China, the pathfinder AVHRR for providing NDVI data, and the NOAA/Climate Diagnostic Center for providing NCEP-NCAR reanalysis data on their Web sites. This study was sponsored by the National Basic Research Program of China under Grant 2007CB411505, the National Key Program under Grant 2007BAC29B02, the Basic Research Program of China under Grant 2003DIB3J120 and the National natural science foundation of China (NSFC) under Grant 40921003.

References

Bounoua L, Collatz GJ, Los SO, Sellers PJ, Dazlich DA, Tucker CJ, Randall DA (2000) Sensitivity of climate to changes in NDVI. J Clim 13:2277–2292

Chen JM, Zhao P, Liu HL, Guo XY (2009) Modeling impacts of vegetation in western China on the summer climate of northwestern China. Adv Atmos Sci 26:803–812. doi:10.1007/s00376-009-9018-2

Dickinson RE, Henderson-Sellers A (1988) Modeling tropical deforestation: a study of GCM land-surface parameterizations. Q J R Meteorol Soc 114:439–462. doi:10.1002/qj.49711448009

Dickinson RE, Shaikh M, Bryant R, Graumlich L (1998) Interactive canopies for a climate model. J Clim 11:2823–2836

Ding MJ, Zhang YL, Liu LS, Zhang W, Wang ZF, Wang B (2007) The relationship between NDVI and precipitation on the Tibetan Plateau. J Geogr Sci 17:259–268

Foley JA, Levis S, Prentice IC, Pollard D, Thompson SL (1998) Coupling dynamic models of climate and vegetation. Glob Change Biol 4:561–579

Frankignoul C, Czaja A, L'Heveder B (1998) Air–sea feedback in the North Atlantic and surface boundary conditions for ocean models. J Clim 11:2310–2324

Goward SN, Markham B, Dye DG, Dulaney W, Yang JL (1991) Normalized difference vegetation index measurements from the advanced very high resolution radiometer. Remote Sens Environ 35:257–277

Gutman GG (1991) Vegetation indices from AVHRR: an update and future prospects. Remote Sens Environ 35:121–136

Hua W, Fan GZ, Zhou DW, Ni CJ, Li XM, Wang YL, Liu YQ, Huang XL (2008) Preliminary analysis on the relationships between Tibetan Plateau NDVI change and its surface heat source and precipitation of China. Sci China Ser D Earth Sci 51:677–685. doi:10.1007/s11430-008-0063-y

Kaufmann RK, Zhou L, Myneni RB, Tucker CJ, Slayback D, Shabanov NV, Pinzon J (2003) The effect of vegetation on surface temperature: a statistical analysis of NDVI and climate data. Geophys Res Lett 30(22):2147. doi:10.1029/2003GL018251

Kim Y, Wang GL (2007) Impact of vegetation feedback on the response of precipitation to antecedent soil moisture anomalies over North America. J Hydrometeorol 8:534–550

Li C, Yanai M (1996) The onset and interannual variability of the Asian summer monsoon in relation to land-sea thermal contrast. J Clim 9:358–375

Li XD, Zhu YF, Qian WH (2002) Spatiotemporal variations of summer rainfall over eastern China during 1880–1999. Adv Atmos Sci 19:1055–1068

Lim Y-K, Cai M, Kalnay E, Zhou LM (2008) Impact of vegetation types on surface temperature change. J Appl Meteorol Climatol 47:411–424. doi:10.1175/2007JAMC1494.1

Liu ZY, Notaro M, Kutzbach J, Liu NZ (2006) Assessing global vegetation-climate feedbacks from observations. J Clim 19:787–814

Los SO (1998) Estimation of the ratio of sensor degradation between NOAA AVHRR channels 1 and 2 from monthly NDVI composites. Geosci Remote Sens 36:206–213. doi:10.1109/36.655330

Nemani RR, Keeling CD, Hashimoto H, Jolly WM, Piper SC, Tucker CJ, Myneni RB, Running SW (2003) Climate-driven increases in global terrestrial net primary production from 1982 to 1999. Science 300:1560–1563

Pielke R, Avissar R, Raupach M, Dolman AJ, Zhen X, Denning AS (1998) Interactions between the atmosphere and terrestrial ecosystems: influence on weather and climate. Glob Change Biol 4:461–475

Tucker CJ, Miller LD (1977) Soil spectra contribution to grass canopy spectral reflectance. Photogramm Eng Rem S 43:721–726

Tucker CJ, Sellers PJ (1986) Satellite remote sensing of primary production. Int J Remote Sens 7:1395–1416

Wang WL, Anderson BT, Entekhabi D, Huang D, Su Y, Kaufmann RK, Myneni RB (2007) Intraseasonal interactions between temperature and vegetation over the boreal forests. Earth Interact 11(18):1. doi:10.1175/EI219.1

Wang YX, Zhao P, Yu RC, Rasul G (2009) Inter-decadal variability of Tibetan spring vegetation and its associations with eastern China spring rainfall. Int J Climatol. doi:10.1002/joc.1939

Wu GX, Liu X, Zhang Q, Qian YF, Mao JY, Liu YM, Li WP (2002) Progresses in the study of the climate impacts of the elevated heating over the Tibetan Plateau. Clim Environ Res 7:184–201 (in Chinese)

Wu GX, Chou JF, Liu YM, Zhang QY, Sun SQ (2003) Review and prospect of the study on the subtropical anticyclone. Chin J Atmos Sci 27:503–517 (in Chinese)

Xue YK (1996) The impact of desertification in the Mongolian and the Inner Mongolian grassland on the regional climate. J Clim 9:2173–2189

Xue F, Guo PW, Yu ZH (2003) Influence of interannual variability of Antarctic sea-ice on summer rainfall in eastern China. Adv Atmos Sci 20:97–102

Yang S, Lau K-M (1998) Influences of sea surface temperature and ground wetness on Asian summer monsoon. J Clim 11:3230–3246

Ye DZ, Gao YX (1979) The meteorology of the Qinghai-Xizang (Tibet) Plateau. Science Press, Beijing, 278 pp

Ye D-Z, Wu G-X (1998) The role of the heat source of the Tibetan Plateau in the general circulation. Meteorol Atmos Phys 67:181–198

Yu RC, Zhang MH, Yu YQ, YM L (2001) Summer monsoon rainfall over mid-eastern China lagged correlated with global SSTs. Adv Atmos Sci 18:179–196

Zhang RH (2001) Relations of water vapor transport from Indian monsoon with that over East Asia and the summer rainfall in China. Adv Atmos Sci 18:1005–1017

Zhang QY, Tao SY (2003) The anomalous subtropical anticyclone in western Pacific and their association with circulation over East Asia during summer. Chin J Atmos Sci 27:369–380 (in Chinese)

Zhang Q, Wu GX, Qian YF (2002) The bimodality of the 100 hPa South Asia high and its relationship to the climate anomaly over East Asian in summer. J Meteorol Soc Jpn 80:733–744

Zhang JY, Dong WJ, Fu CB (2005) Impact of land surface degradation in northern China and southern Mongolia on regional climate. Chin Sci Bull 50(1):75–81

Zhang RH, Wu BY, Zhao P, Han JP (2008) The decadal shift of the summer climate in the late 1980s over East China and its possible causes. Acta Meteorol Sin 66:697–706

Zhao P, Chen LX (2001a) Interannual variability of atmospheric heat source/sink over the Qinghai-Xizang (Tibetan) plateau and its relation to circulation. Adv Atmos Sci 18:106–116

Zhao P, Chen LX (2001b) Climatic features of atmospheric heat source/sink over the Qinghai-Xizang Plateau in 35 years and its relation to rainfall in China. Sci China Ser D Earth Sci 44:858–864

Zhao P, Chen JM, Xiao D, Nan SL, Zou Y, Zhou BT (2008) Summer Asian-Pacific oscillation and its relationship with atmospheric circulation and monsoon rainfall. Acta Meteorol Sin 22:455–471

Zhao P, Zhang XD, Li YF, Chen JM (2009) Remotely modulated tropical-North Pacific ocean-atmosphere interactions by the South Asian high. Atmos Res 94:45–60. doi:10.1016/j.atmosres.2009.01.018

Zheng YQ, Qian YF, Miao MQ (2002) The effects of vegetation change on the regional climate I: the simulation results. Acta Meteorol Sin 60:1–16 (in Chinese)

Zhu JH, Wang SW (2001) 80a-oscillation of summer rainfall over the east part of China and East-Asian summer monsoon. Adv Atmos Sci 18:1043–1051

Zhu YX, Ding YH, Xue HG (2007) The decadal relationship between atmospheric heat source of winter and spring snow over Tibetan Plateau and rainfall in East China. Acta Meteorol Sin 65:946–958 (in Chinese)